Grain size, composition, porosity and permeability contrasts within cross-bedded sandstones in Tertiary fluvial deposits, central Spain

CHRISTEL A. HARTKAMP,* JOSÉ ARRIBAS† *and* AMPARO TORTOSA†

**Faculty of Mining and Petroleum Engineering, Delft University of Technology, P O Box 5028, 2600 GA Delft, the Netherlands*

†Departamento de Petrologia y Geoquimica, Facultad de Ciencias Geologicas, Universidad Complutense, 28040 Madrid, Spain

ABSTRACT

Permeability measured wit ha portable probe permeameter on outcrops of cross-bedded sandstones ranges between 0·9 and 19 D. The highest permeability (2–19 D with an average of 8·5 D) occurs in the coarsest grained foreset laminae (CFL), intermediate values (2–12 D with an average of 5·3 D) occur in finer grained foreset laminae (FFL) and the lowest values (0·9–10 D with an average of 4·8 D) occur in bottomset layers (BL). In the cross-beds the average grain size ranges from medium grained sand in the CFL to fine grained sand in the FFL and BL. In all three subfacies, the average size of the primary pores is approximately 1ϕ unit smaller than the average grain size. The abundance of unstable carbonate clasts correlates with increasing average grain size, micritic clasts being most abundant in the CFL. Conversely, quartz content increases with decreasing grain size and is highest in the FFL and BL. Diagenetic destruction of primary porosity by compaction and cementation, as well as generation of secondary porosity through dissolution, were controlled by the original mineralogical composition of the sand. Contrasts in grain size determine the primary pore size contrasts and differences in composition between CFL, FFL and BL. Permeability contrasts reflect variations in average primary pore size rather than differences in total porosity. Probe permeability contrasts between CFL, FFL and BL depend on contrasts in average pore size and contrasts in mineralogical composition between the subfacies.

INTRODUCTION

Many studies have related permeability measured by a probe permeameter at outcrop to the sampled sedimentary facies (e.g. Chandler *et al.*, 1989; Dreyer *et al.*, 1990; Hartkamp & Donselaar, 1993). Most studies have concentrated on permeability variations on genetic-unit scale. In a laboratory setting, probe permeameter measurements can be made on a very fine-scale grid, enabling statistically valid comparisons to be made between the permeability distributions of individual laminae in cross-stratified units (grid point spacing of 5 mm; Hurst & Rosvoll, 1991). However, there are few studies that directly combine detailed probe permeametry at outcrop with microscopic textural and mineralogical observations.

In the past few decades, experimental, theoretical and semi-empirical relations have been established between pore and textural characteristics (e.g. grain size, sorting, specific surface of grains) of sands and sandstones with permeability (e.g. Kozeny, 1927; Carman, 1937; Beard & Weyl, 1973; van Baaren, 1979). Textural properties are basically determined by the primary mineralogical composition and the physical processes of sedimentation, but may be affected by subsequent burial history (e.g. physical compaction, mineralogical alteration and cementation; Pittman, 1979). Studies on reservoir sandstones have provided a more detailed insight into the dependence of permeability on porosity alteration as a result of diagenesis. For example, Ehrenberg (1990) studied North Sea reservoir sandstones and found that both finer grain size and higher mica content were associated with lower permeability. Differences in

mineralogical composition between laminae within cross-stratified reservoir sandstones have been observed by Hopkins *et al.* (1991) permeability contrast of one order of magnitude between the laminae. Hurst & Rosvoll (1991) determined a permeability contrast of 1–3 orders of magnitude between laminae within a cross-bed of shallow marine origin in a lightly consolidated sandstone; they assumed that the variations in permeability reflected primary depositional characteristics.

The present study focuses on quantification of permeability variations in cross-bedded sandstones. The purpose of this paper is to document the depositional characteristics that affect contrasts in permeability between adjacent foreset laminae and between foreset and bottomset of cross-beds in well exposed distal fluvial fan deposits of Late Oligocene to Early Miocene age (Loranca Basin in central Spain). Probe permeameter measurements are compared with textural and compositional parameters. The studied sandbodies are lightly consolidated and have retained most of their primary depositional features (Diaz Molina *et al.*, 1989).

GEOLOGICAL SETTING AND FACIES DESCRIPTION

Sandstones of Middle to Late Tertiary age in the Loranca Basin of central Spain provide the data for this study (Fig. 1). Fluvial, molasse-type, sandstones from two coalescing systems filled the Loranca depression during the Late Oligocene to Early Miocene (Diaz Molina *et al.*, 1989). The source areas of these fluvial sediments are the Mesozoic clastic and carbonate sequences of the Iberian mountain range. Channel sandbodies were formed by low and high sinuosity rivers and enclosed in fine grained floodplain sediments. Large scale trough cross-bedding is ubiquitous (Diaz Molina *et al.*, 1985).

The trough cross-bedded sedimentary structures were formed by large scale ripple migration over the channel floor and the depositional slope of the inner bank. The trough cross-beds have lengths of up to 20 m, thicknesses of 20–40 cm and widths of 80 cm to 2 cm. Two different facies are distinguished: the bottomset and the foreset. The bottomset layer (BL) has formed in front of migrating ripples and consists of fall-out and suspension-load sediment. Foreset deposits consist of laminae that formed by grains avalanching down the leeside of ripples. The inclined foreset laminae are preserved in sequence in the sandbodies and are a record of successively earlier positions of the leesides. The grains are sorted during avalanching, resulting in distinct coarse (CFL) and

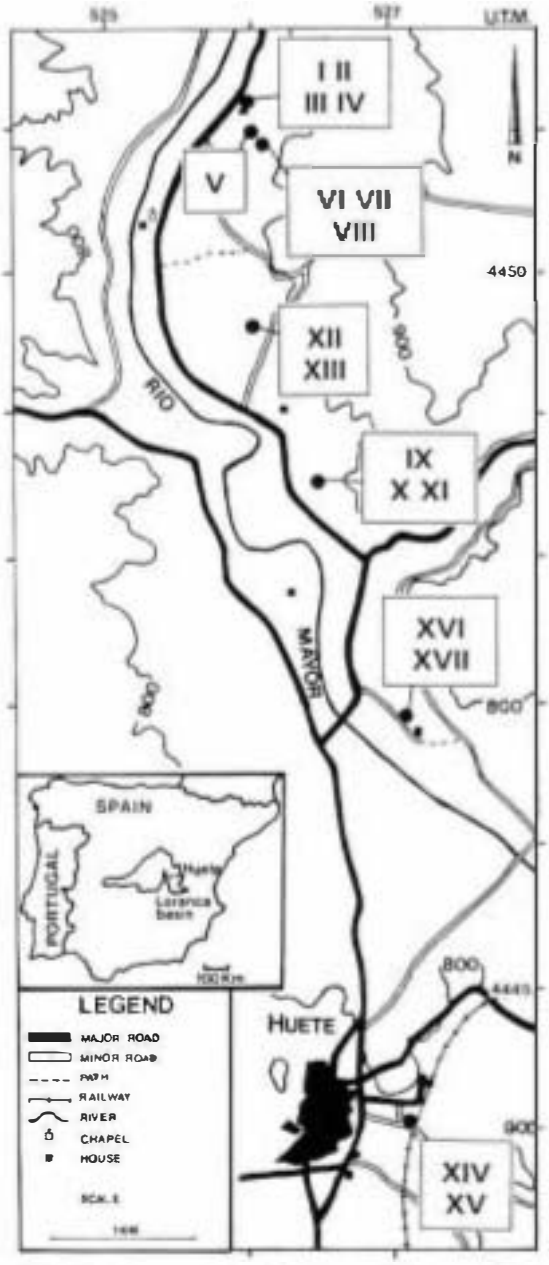

Fig. 1. Location map of the study area in the Loranca Basin of central Spain. Studied outcrop locations are marked from I–XVII.

fine grained (FFL) laminae that range between 2 mm and 1·2cm in thickness. Usually, there is a regular and systematic pattern of variation in medium grain size with respect to the successive cross-strata.

METHODOLOGY

Petrography

A total of 34 plugs, each 2 in (5·08 cm) in diameter, were taken perpendicular to bedding from 17 outcrop locations (Figs 1 and 2A–C). Probe permeability measurements were taken prior to coring and this technique provided us with undisturbed plugs of which the measured locations, orientations, exact sedimentological details, and probe permeability data were known at 90° to layering. Thin sections of the plugs were made following impregnation with blue Araldite and a qualitative evaluation was made (Fig. 2C, D), and nine thin sections were selected and used for optical petrographical analysis. In each thin section, the coarser grained foreset laminae (CFL), the finer grained foreset laminae (FFL) and the bottomset layer (BL), if present were studied separately. The parameters studied comprise mineralogical composition, grain size distribution and porosity.

Petrographical analysis involved counting a total of 3300 points in each plug sample. For each subfacies (CFL, FFL and BL), 400 points were counted of framework and cement type, 400 points were counted of pore type and size and a further 300 points were counted for grain size determination. In foreset laminae the point count parameters were counted parallel to the dip (Fig. 2D). In bottomsets the parameters were counted perpendicular to the depositional surface, to account for any anisotropy in texture that may be apparent in bottomsets (Joplin, 1965). In some samples, bottomsets display well developed, fine and coarse grained laminae; in these samples point counting was done parallel to the depositional surface in order to count coarse and fine grained laminae separately (BL–C and BL–F).

Maximum diameters of pore size and grain size were counted in ϕ unit intervals ($-\log_2$ of the diameter (mm), Pettijohn *et al.*, 1973). Mean values of grain size or pore size were used in the correlations with permeability. Sorting ($So = \phi$ standard deviation) was calculated in accordance with Folk (1980). Framework composition was analysed in petrographical groups as defined by Zuffa

analysis (primary and secondary porosity) was carried out on the basis of the criteria defined by Schmidt & McDonald (1979).

Permeability

The probe permeameter (minipermeameter) was developed for measuring the steady state permeability of rock and unconsolidated sand by Eijpe & Weber (1971). Sutherland *et al.* (1991) recommended codes of practice that are applicable to the variety of instruments currently available and given details of the measurement principles, apparatus, measurement procedure and quality control for probe permeametry. The apparatus and the measurement techniques used for this study are described in detail by Hartkamp & Donselaar (1993) and are only summarised here. The probe permeameter consist of three units, a nitrogen gas source, a flow meter unit and a probe. The probe is pressed against the rock surface with a controlled force (Sutherland *et al.*, 1991). At a constant pressure, nitrogen is passed through a small opening in the probe into the rock and the flow rate is recorded when a steady state is reached (after 10 s). Leakage between the rock and the probe is prevented by an elastic, closed-cell neoprene rubber. The inlet opening of the probe (radius of 1 mm) determines the measured rock volume (Goggin *et al.*, 1988), which is estimated to have a radius and depth of 4 mm. Where the thickness of laminae is less than the measurement radius, the measured permeability is an average value defined by the unknown permeabilities of more than one lamina (Halvorsen & Hurst, 1990).

Flow rate is converted into permeability using a calibration curve (Fig. 3). This calibration curve was established in the Dietz laboratory of Delft University of Technology (the Netherlands) using a set of 99 natural and artificial homogeneous sandstone plugs, the permeabilities of which ranged from 0·1 to 14 000 mD. An extensive description of the principles, calibration, response, reliability and accuracy of the equipment used for this study is presented by Hartkamp (1993).

The outcrop face was carefully prepared using a steel brush to remove the superficial weathering crust and, subsequently, using a soft brush to remove the first few centimetres of the friable sandstone underneath the crust in order to remove dust and flatten the surface.

A total of 2600 measurements were made on cross-beds at 17 outcrop locations and statistically analysed.

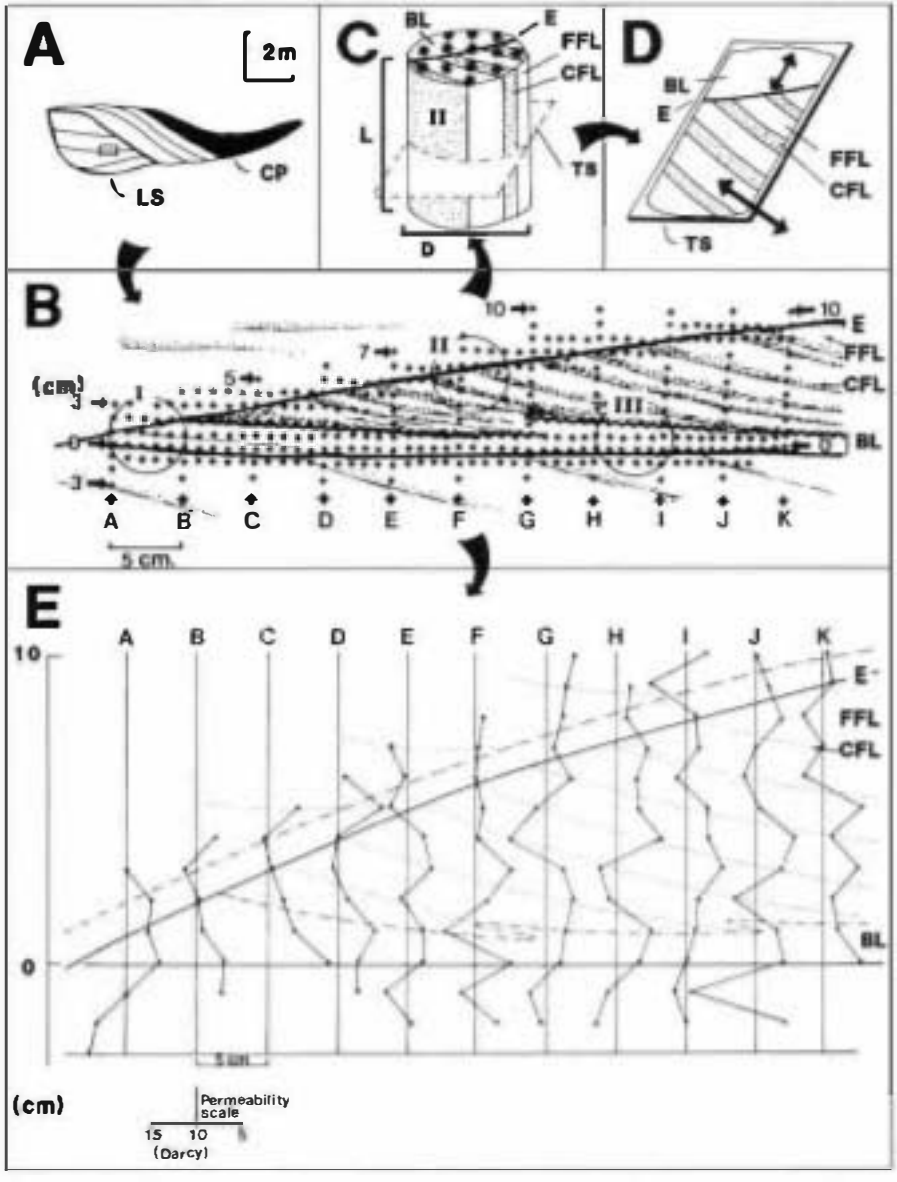

Fig. 2. (A) A schematic cross-section of a laterally stacked sequence of adjacent point bar deposits (LS) and channel abandonment deposits represented by a clay plug (CP). ●utcrop sample location VI is indicated by the rectangular box. (B) Drawing of the sampled cross-bed set of location VI. Coarser grained foreset laminae (CFL) are stippled, finer grained foreset laminae (FFL) are unornamented and the bottomset layer (BL) is the unornamented zone parallel to the bold erosion surface (E) and the undulating line. Circles indicate core plug locations (I, II and III). The grid used for probe permeameter measurements is indicated by asterisks (vertical grid spacing is 1 cm, horizontal grid spacing between columns A and K is 5 cm, with additional grid points 1 cm apart. (C) Example of core plug II with a length (L) of 6 cm and a diameter (D) of 5·08 cm. Inclined foreset laminae are presented as CFL (stippled) and FFL (unornamented). BL is unornamented and overlies the erosion surface (E). Asterisks indicate probe permeameter sample points. TS is the imaginary cross-section for the thin section. (D) Example of thin section (TS) with foreset laminae CFL (stippled) and FFL (unornamented), the erosion surface (E) and overlying bottomset (BL). Arrows indicate the point count directions in the foreset (CFL, FFL) and in the bottomset (BL). (E) Example of permeability pattern of outcrop location VI; the dotted lines indicate inclined foreset laminae directions (CFL, FFL), the dashed line indicates the boundary between forest and bottomset (BL) and the black line indicates the erosion surface (E).

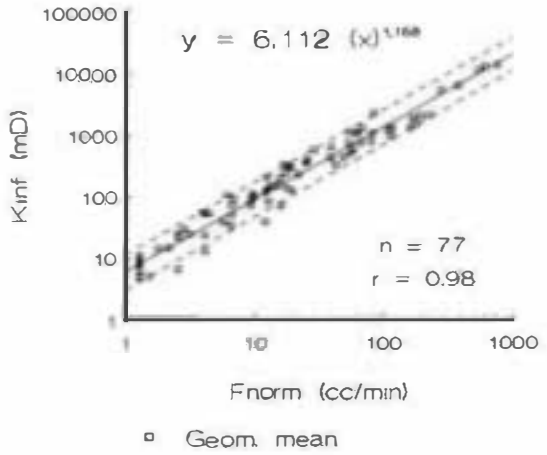

Fig. 3. Calibration graph of the normalized flow rate (F_{norm}) measured by probe permeameter versus the infinite plug permeability (K_{inf}) (Hassler-sleeve) for the highest range in permeability (5 to 14 000 mD). Data represent geometrical averages of four probe measurements taken at each end side of a core plug. The power regression relationship of the best-fit correlation (continuous line) is presented, together with the total number (n) of core plugs involved and the correlation coefficient (r). The 80% confidence intervals are indicated by dashed lines and show an error of calibration of a factor 1·6.

From this total only 525 measurements from nine locations were ultimately used for the comparative study between petrography and permeability. This restriction of data was determined by the limited amount of locations from which thin sections could be prepared successfully. Thus, only 25 data points are presented in Table 1, of which anomalous points were eliminated from the subsequent correlation graphs.

Measurements were taken on a grid with a vertical spacing of 1 cm and a horizontal spacing of 5 cm. Total column height ranged between 10 and 50 cm, and the total number of columns ranged between 6 and 15. On key horizons (e.g. bottomsets) additional rows were measured, with a horizontal and vertical grid distance of 1 cm (Fig. 2B, E).

The permeability data have been grouped as CFL, FFL and BL data on the basis of sedimentological characteristics at the points of measurement (Fig. 2E). The resulting three data sets were analysed using standard population statistical techniques. Histograms and cumulative frequency plots were used to characterize the distributions of datasets and sub-datasets, from which the optimal averaging technique was judged.

RESULTS

Petrography

The cross-bedded sandstone is generally very fine to coarse grained and moderately well sorted (So = 0·6–0·9, Table 1). The grains are usually subangular to subrounded. The framework is composed of three main groups of gains: (1) non-carbonate extrabasinal grains (NCE), (2) carbonate extrabasinal grains (CE) and (3) carbonate intrabasinal grains (CI) (see Table 1).

(1) NCE comprise approximately 75% of the framework, and are mainly monocrystalline and polycrystalline quartz and K-feldspar. Monocrystalline quartz grains usually show a non-undulatory extinction. The grains are typically irregularly overgrown, and in some cases contain anhydrite inclusions. These features are indicative of provenance from a sedimentary source area (Arribas & Arribas, 1991). K-feldspar is not abundant (less than 11%), and has inherited overgrowths and filled grain fractures. Partial dissolution of K-feldspar grains is common.

(2) CE are limestone and dolostone fragments, displaying micritic (CEm) and sparitic (CEsp) textures. CE grains make up 10–35% of the total rock volume.

(3) CI are micritic grains and oncolite fragments. Micritic grains have a homogeneous texture and sometimes contain fragments of *Characeas* sp. and ostracods. In general, they are larger than extrabasinal grains. The intrabasinal clasts were soft and unstable at the time of deposition and often have been deformed by compaction. The percentage of CI grains in the framework ranges from 5 to 25%.

The composition of the sandstones is shown in Fig. 4. All plotted points fall in the field in which extrabasinal grains dominate (Fig. 4A). The average composition of these extrabasinal grains is lithoarenitic (Fig. 4B). In agreement with the composition of the sandstone and the sedimentary nature of the rock fragments, the deposits are defined as sedimentoclastic (cf. Ingersoll, 1983). In the NCE–CE–CI diagram (Fig. 4A) samples from each outcrop location form separate clusters, indicating that each sample location has a slightly different bulk composition. In the QFR diagram (Fig. 4B), in which intrabasinal grains are not included, the separation between different outcrops is less clear. The different clusters of data vary

Table 1. Texture, composition and permeability of analysed sandstones.

Sample	Texture						Composition (%)						Permeability (D)			
	Average grainsize (ϕ)	Sorting	Primary porosity (%)	Secondary porosity (%)	P1 pore size (ϕ)	P2 pore size (ϕ)	Q	K-feldspar	CEm	CEsp	Cl	Carbonate cement	Range	Average	SD	n
CFL																
VI.2	1·42	0·80	21·2	10.8	2·26	1·10	64·3	10·0	6·3	12·6	5·6	0·9	8·20–15·45	10·72	1·77	43
IX.1	1·51	0·62	30·0	4·6	2·26	1·89	65·5	8·6	6·0	14·3	4·0	0·6	6·08–11·93	8·49	1·56	10
IX.2	1·75	0·81	24·6	7·2	2·75	1·31	59·6	10·3	9·3	14·9	5·6	0·0	6·80–10·01	8·59	1·33	7
XII.1	1·94	0·79	25·0	6·0	2·62	1·72	56·2	5·6	6·6	21·6	8·3	1·3	2·13–6·76	4·38	1·66	4
XIII.2	2·02	0·72	23·6	4·2	2·94	2·11	48·6	7·0	9·0	24·2	10·3	0·6	4·11–5·52	4·90	0·51	4
XIV.1	2·32	0·99	14·8	3·8	2·74	1·18	37·0	6·5	10·6	18·6	25·0	0·9	7·00–15·10	10·63	2·09	14
XV.1	1·57	0·74	19·4	10·2	2·46	0·66	57·1	5·9	4·3	11·5	16·8	4·2	3·41–9·83	5·73	1·39	30
XV.2	2·69	0·69	16·4	3·4	3·62	2·14	65·6	3·6	4·6	11·6	13·0	4·0	8·16–11·54	9·97	1·16	8
XVII.1	2·20	0·82	19·8	5·6	2·45	1·48	67·9	5·0	4·6	6·3	13·3	2·6	6·12–18·86	12·68	3·3	28
FFL																
VI.2	2·35	0·69	18·0	7·2	3·22	2·01	68·5	3·6	9·6	10·3	6·0	1·6	4·84–9·67	7·07	1·22	34
IX.1	2·24	0·71	24·4	4·8	3·20	2·06	69·6	3·0	6·3	13·0	4·6	3·3	3·81–6·43	4·93	0·83	8
IX.2	2·67	0·82	17·8	3·2	3·34	2·05	59·6	6·0	10·0	10·6	10·3	3·3	4·11–6·28	5·51	0·69	7
XII.1	2·29	0·69	22·2	5·2	3·37	2·03	62·6	4·0	12·6	12·0	8·3	1·3	2·77–5·10	3·92	0·65	14
XIII.2	3·09	0·76	21·5	2·9	3·84	2·42	57·6	4·6	10·6	15·3	10·0	1·6	1·72–4·31	3·39	0·72	27
XIV.1	2·54	0·92	16·6	7·0	3·30	2·40	56·2	3·6	11·6	7·0	19·0	2·3	2·70–8·94	6·07	2·07	28
XVII.1	2·45	0·78	19·2	8·6	3·07	2·08	56·6	4·0	1·6	6·6	18·0	3·9	2·10–12·01	5·99	2·09	55
BL																
VI.2	2·14	0·67	18·1	8·7	3·10	1·79	62·5	5·6	7·6	13·6	5·3	4·9	3·01–10·60	7·28	1·42	36
IX.1	2·53	0·72	22·2	5·0	3·30	1·73	62·9	3·0	6·0	15·3	7·0	5·6	2·47–5·93	3·74	1·04	9
XII.1	2·92	0·74	21·0	5·8	3·50	1·44	54·3	3·6	6·0	22·0	9·6	4·3	2·15–6·89	3·95	1·14	26
XIII.2	2·97	0·71	20·8	5·4	3·60	1·83	58·9	4·6	6·3	20·0	5·6	4·3	1·62–5·95	3·72	1·25	24
XIV.1	2·95	0·78	18·8	9·2	2·98	1·17	57·6	4·0	8·0	15·3	7·0	8·0	1·36–10·51	6·00	1·82	43
XV.1-C	2·55	0·95	16·8	3·0	3·12	1·90	52·3	5·3	5·6	11·0	23·0	1·6	2·47–5·10	3·73	0·68	26
XV.1-F	2·36	1·05	18·2	5·4	2·54	1·43	55·6	3·6	7·6	14·6	15·3	2·3	1·72–8·03	4·77	1·91	22
XV.2-C	2·72	0·86	20·8	4·2	2·71	2·36	51·6	5·6	5·2	11·5	24·7	1·3	4·09–7·50	6·06	1·06	8
XV.2-F	3·26	0·96	22·6	3·6	3·73	2·86	56·0	4·0	4·0	13·0	22·0	1·0	0·93–5·01	3·84	0·85	10

Sorting is the phi standard deviation (Folk, 1980). Composition is subdivided into quartz (Q), K-feldspar, micritic carbonate extrabasinal grains (CEm) and sparitic carbonate extrabasinal grains (CEsp), carbonate intrabasinal grains (Cl) and carbonate cement. The range, arithmetic average, standard deviation (SD) and number of measurements (n) of permeability is presented.

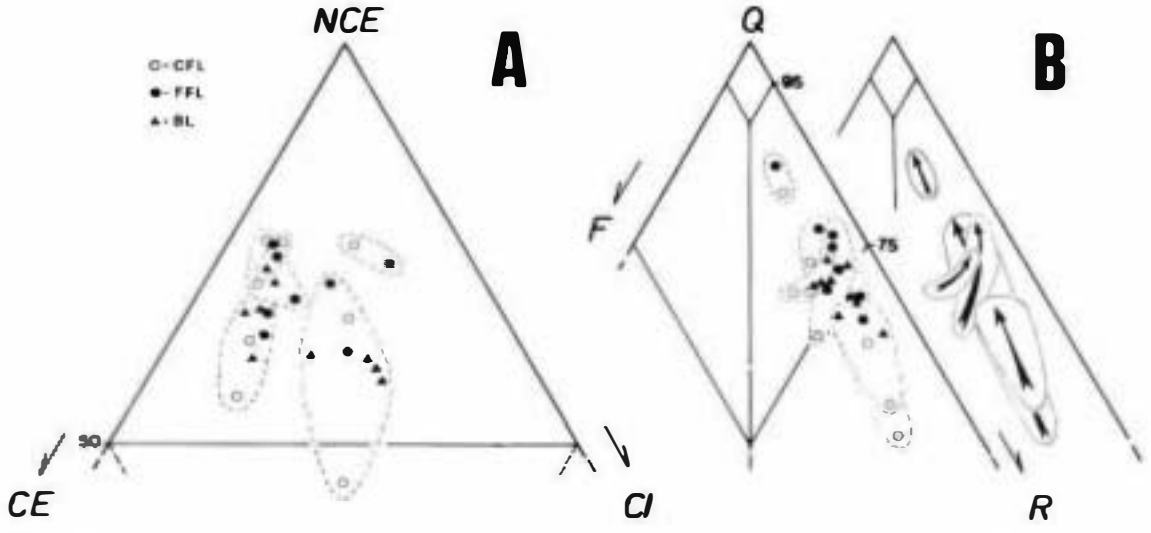

Fig. 4. Framework composition of sandstones: (A) in an NCE–CE–CI diagram (after Zuffa, 1980; (B) in a Q–F–R diagram (after Pettijohn *et al.*, 1973). Samples of a corresponding outcrop location are clustered. Arrows indicate variation in composition from coarser to finer grained subfacies in a cross-bedded set. NCE, non-carbonate extrabasinal; CE, carbonate extrabasinal; CI, carbonate intrabasinal; Q, quartz; F, feldspar; R, rock fragments.

in the ratio between quartz and rock fragments, reflecting small differences in provenance between the various outcrop locations.

Porosity is interpreted to be mainly of primary origin. Primary porosity ranges from 16·4 to 30% (Table 1). Primary porosity is characterized by interparticle pores, with a poresize distribution closely related to the grain size (Fig. 5). The average primary pore size is approximately 1 ϕ unit smaller than the average grain size.

Diagenesis

Diagenesis of the sandstones includes mechanical and chemical compaction, cementation and generation of secondary porosity. Mechanical compaction mainly affected intrabasinal micritic grains and produced deformed and disintegrated grains. Chemical compaction affected hard micritic grains and some intrabasinal grains (oncolites), which often have concavo-convex contacts with siliciclastic grains, without deformation of internal textures. Cementation has generally not been intense (less than 4%; Table 1) and cements consist mainly of calcite overgrowths around monocrystalline carbonate grains. Locally, equant calcite mosaics are present. From the textural relationship between deformed soft grains and the undeformed calcite cement, it is concluded that cementation postdates compaction.

Secondary porosity generation is the last diagenetic process to have affected the sandstones. Secondary porosity is characterized by the presence of oversized

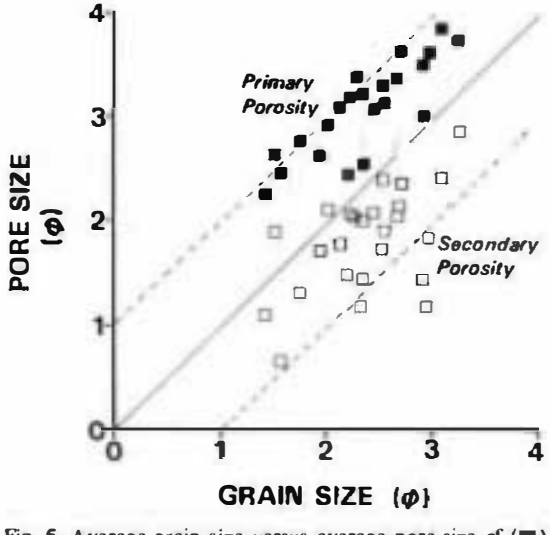

Fig. 5. Average grain size versus average pore size of (■) primary and (□) secondary porosity.

pores (Fig. 6A). Features indicative of secondary porosity, such as inhomogeneity of packing (Schmidt & McDonald, 1979), are common. Micritic grains have highly corroded edges. Intragranular dissolution pores affect the dissolution of mainly intrabasinal micritic grains. Secondary pore size is less well correlated with grain size than in the case of primary pore size (Fig. 3), and shows a larger scatter of data points with average pore sizes mainly 1ϕ unit larger than the average grain size.

Compaction is the most intense diagenetic process that has modified primary porosity by deformation of soft grains as a result of mechanical compaction (Fig. 6B) and the interpenetration of hard grains by chemical compaction (cf. Rittenhouse, 1971; Mwa. & Beard, 1980). A clear decrease in primary porosity

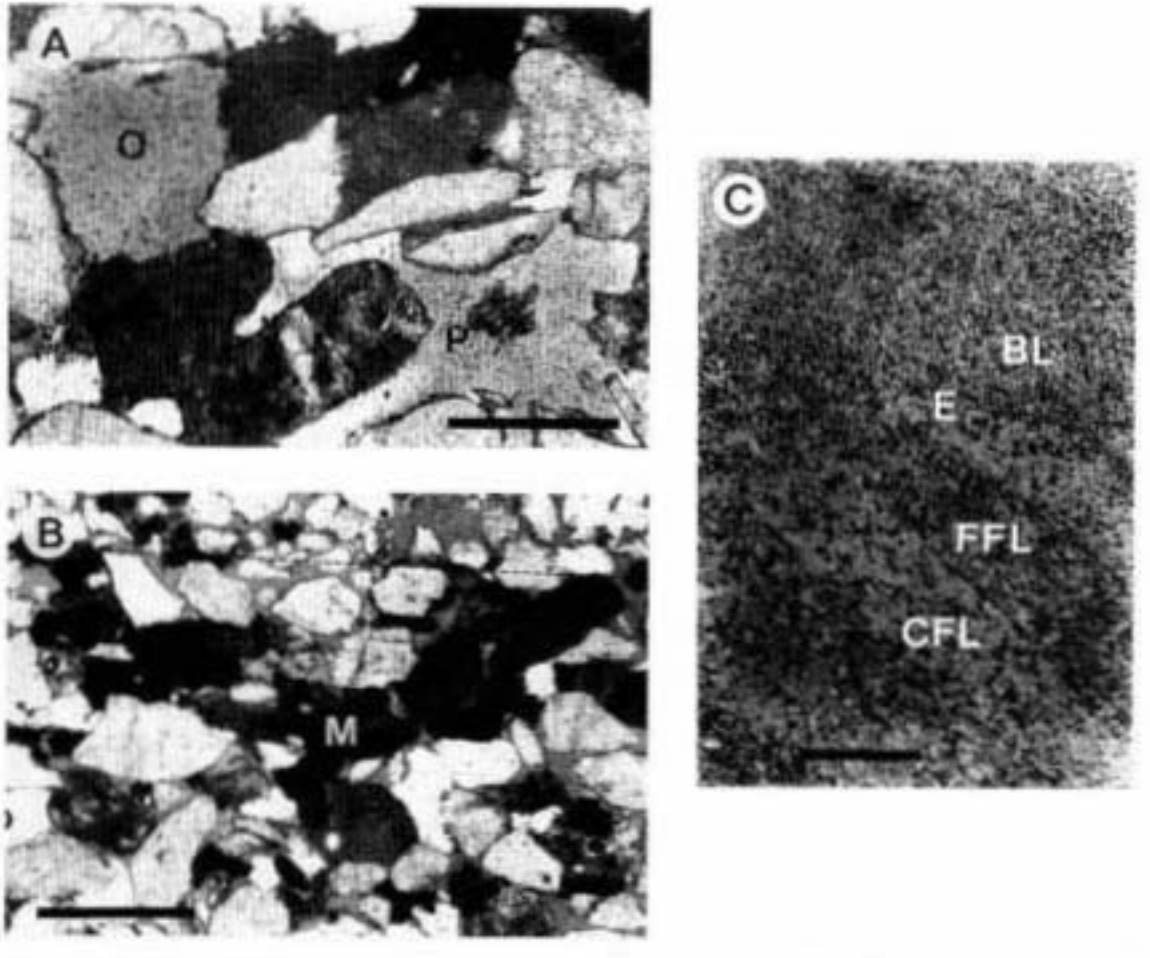

Fig. 6. (A) Photomicrograph in plane-polarized light of sample XII.1 (scale bar = 0·25 mm). Oversized pores of secondary origin created by complete (O) and near-complete (P) dissolution of carbonate grains. Note compaction of micritic grains (dark grey). Light grey areas represent void space. (B) Photomicrograph in plane-polarized light of sample XII.2 (scale bar = 0·5 mm). Reduction of primary porosity by mechanical compaction of micritic intrabasinal grains (M). Light grey areas represent void space. Note sharp boundary between CFL (lower part) and FFL (upper part) indicated by a dashed line. (C) Photomicrograph in plane-polarized light of sample VI.2 (scale bar = 1 cm) of upper part of a foreset with coarser (CFL) and finer (FFL) grained laminae, overlain by a fine grained bottomset (BL) of the vertically stacked cross-bedded sets. Sharp boundaries between the subfacies CFL and FFL are indicated by dashed lines. The erosion surface (E) that forms the boundary between the lower foreset (CFL and FFL) and the overlying BL is indicated by a continuous line.

was found in sandstones with a high percentage of micritic grains (Fig. 7A). This relationship (correlation coefficient $r = -0{\cdot}555$) is obscured by later diagenetic processes such as cementation and secondary porosity generation. It is assumed that secondary porosity merely resulted from dissolution of micritic grains. Thus, by adding the percentage of secondary porosity to the percentage of micritic grains, an estimate of the original micritic grain content is obtained. The percentage of cement, resulting in a reduction of the primary porosity, may be added to the percentage of primary porosity (horizontal axis of the graph), yielding the percentage of pre-cementation porosity (Fig. 7B). Thus, the original porosity of a sandstone with an original framework composition of approximately 40% carbonate micritic grains is reduced to near 15% by compactional processes. This fact outlines the relevance of sandstone composition on primary porosity reduction.

Contrasts in petrography

Boundaries between the different subfacies CFL, FFL and BL are often very sharp (Fig. 6C). It can be observed that the CFL is characteristically coarser grained (medium grained sand) than the FFL and BL (fine grained sand). Sorting of CFL has a wider range (0·62–0·99, well to poorly sorted) than the FFL (0·69–0·92, moderately to well sorted). The bottomset sands (BL) are generally not as well sorted as the FFL (sorting of BL ranges between 0·67 and 1·05). In some cases, bottomsets are better sorted than the foreset laminae. The three subfacies have similar lower limits of primary porosity (16·2–16·8%, the value of 14·8% is considered anomalous), but differ in their upper limits (CFL: 30%, FFL: 24·4% and BL: 22·2%). As pore size (primary and secondary) is directly related to average grain size (see Fig. 5), the pores of CFL are larger than those in FFL and BL.

A significant difference in composition between coarser grained (CFL) and finer grained (FFL + BL) subfacies of individual cross-bedded sets has been observed. The QFR diagram (see Fig. 4B, direction of the arrows) shows that the percentage of quartz grains increases with decreasing grain size. Contrasts in the quantity of micritic grains between the CFL, FFL and BL of individual cross-bed sets result in contrasts of primary porosity evolution and development of secondary porosity between the subfacies (Table I).

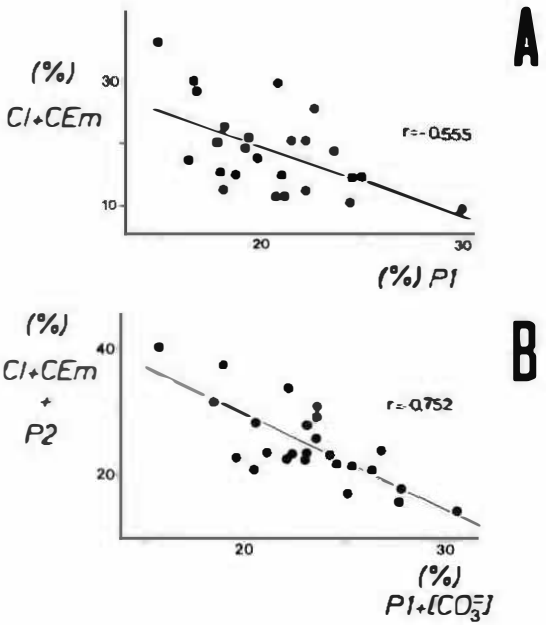

Fig. 7. (A) Percentage of intrabasinal (CI) and extrabasinal carbonate micritic (CEm) grains versus percentage of primary porosity (PI). (B) Percentage of secondary porosity (P2) added to CI + CEm) versus carbonate cement percentage ($CO_3^{=}$) added to (PI).

Contrasts in permeability

The 2600 outcrop probe permeameter measurements range between 0·5 and 20 D. In cross-bedded sets where the range in grain sizes is small, the range of permeability is also small. Population statistics prove the independence of the different subfacies (H & Donselaar, 1993). On the basis of histograms and cumulative frequency plots of permeability data populations and subpopulations (e.g. Fig. 8), the following observations were made. (1) Data populations show approximately normal, log-normal or bulk (frequency maxima over several permeability classes) distributions. (2) Subpopulations (i) are in general approximately normally distributed (Gaussian distributions), but log-normal distributions also occur; (ii) foreset data distributions often show two distinct frequency maxima (bimodality according to CFL and FFL data), with a 2–5 D difference; frequency of bottomset (BL) data often fall in the same class as the lower permeability peak (FFL) of the foreset data distribution (Hartkamp, 1993). From these observations it is concluded that the optimal procedure for calculating the mean of data subpopulations, corresponding to CFL, FFL and BL, is the

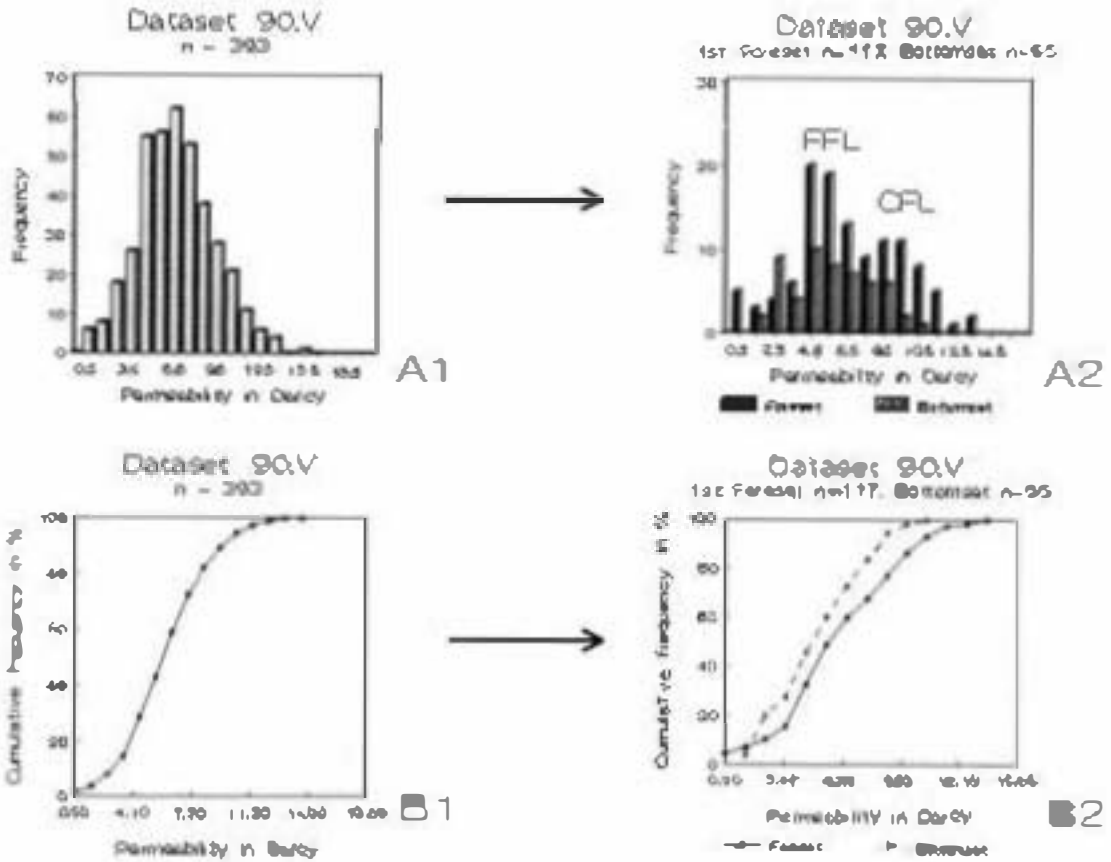

Fig. 3. Example of frequency distributions of (A1) total dataset 90.V and (A2) sub-datasets, fossil and bioturbated, of one cross-bed. Example of cumulative frequency curves of (B1) total dataset 90.V and (B2) sub-datasets, foreset and bottomset, of one cross-bed. The total dataset has an approximately normal distribution. The sub-datasets of the foresets show a bimodal character, according to FFL and CFL data.

and kinetic sieving method (Giménez & Ascaso, 1981). The occurrence of approximately normally distributed permeability data related to 'homogeneous' sand types (bedding, sedimentary structures) is confirmed by other studies (e.g. Jensen et al., 1987; Gibbons et al., 1991, Tyler et al., 1991).

The frequency distributions of the arithmetic average permeability of CFL, FFL and BL data of all studied cross-beds (17 locations) are presented in Fig. 9. On average, contrasts between subfacies are 2:1:25:1 (CFL:FFL:BL). The specific permeability ranges, averages and standard deviations of the petrographically characterized cross-beds (525 measurements) are presented in Table 1. Standard deviations of CFL represent the largest variation in measurements, while standard deviations of FFL specify the smallest range in measured values.

DISCUSSION

Permeability in sandstones is in general linearly related to porosity on a log-normal scale (Jensen, 1990). By contrast, in Fig. 10 very vague trends occur between total porosity, primary and secondary porosity, and the permeability of the studied sandstones. The data show a wide spread (correlation coefficients for best-fit lines were 0.02 of total porosity, – 0.16 of primary porosity and 0.24 of secondary porosity). Figure 11 shows that average permeability correlates

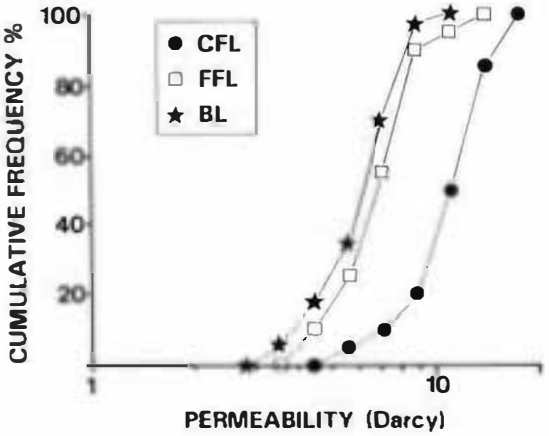

Fig. 9. Cumulative frequency distributions of arithmetic average permeability of CFL, FFL and BL data of all 17 outcrop locations (average permeability of CFL = 17, FFL = 17 and BL = 25). On average, contrasts are 2:1·25:1 (CFL: FFL: BL).

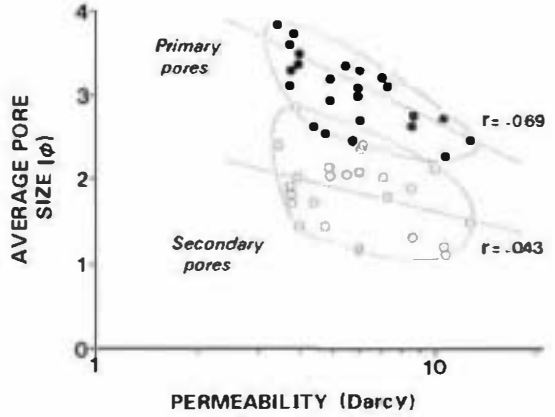

Fig. 11. Average pore size of primary (●) and secondary (○) pores versus permeability.

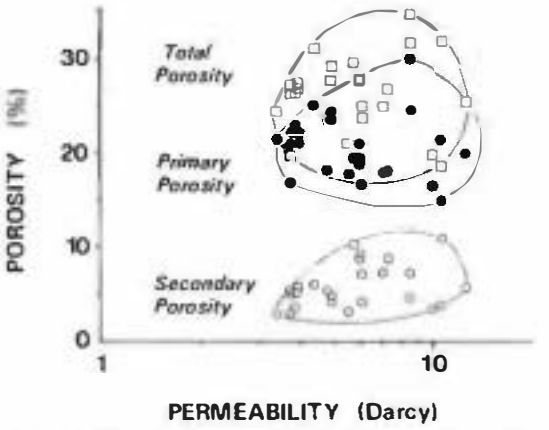

Fig. 10. Primary (●), secondary (○) and total (□) porosity versus permeability.

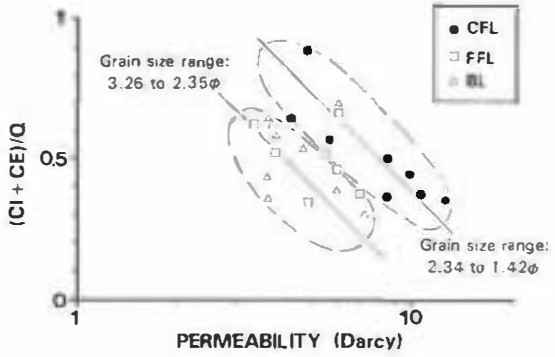

Fig. 12. Sandstone composition [(CI + CE)/Q index] versus permeability with samples grouped as a function of grain size. Note the relevance of provenance (sandstone composition) and grain size on permeability. CI, carbonate intrabasinal, CE, carbonate extrabasinal; Q, Quartz.

well with the average pore size of primary pores, although the correlation with the average pore size of secondary pores is less clear. However, permeability clearly decreases with decreasing average pore size. From a comparison of Figs 10 and 11 it can be inferred that permeability depends more on average pore size than on total porosity.

To emphasize the effect composition exert on permeability, a graph of permeability versus composition (ratio of carbonate to quartz grains) is presented in Fig. 12. The different grain sizes are reflected in the separation of the generally coarser grained CFL and the generally finer grained FFL and BL. For both clusters a clear correlation exists between a carbonate to quartz with increasing permeability. Figure 12 shows that permeability depends primarily on: (1) mineralogical composition and related diagenetic processes (y = axis) and (2) the grain size.

CONCLUSIONS

1. In the cross-beds, average grain sizes range from medium grained sand in the coarser grained foreset laminae (CFL) to fine grained sand in the finer grained foreset laminae (FFL) and bottomset (BL). The sand is on average moderately well sorted ($So = 0{\cdot}6$–$0{\cdot}9$).
2. The average size of primary pores is approximately 1ϕ unit smaller than the average size of the pore-forming grains. The secondary pores (oversized pores) are approximatelyh 1ϕ unit larger than the average grain size.
3. The differences in framework composition between the different outcrop locations are a result of small differences in provenance. Compositional contrasts between the subfacies of a cross-bedded set are related to grain size. Coarser grained foreset laminae (CFL) have a larger amount of carbonate intra- and extra-basinal grains than do the adjacent finer grained laminae (FFL) and bottomsets (BL).
4. The abundance of micritic grains is decisive in the course of diagenesis, controlling the primary porosity reduction by compaction and secondary porosity generation. Contrasts in the quantity of micritic grains between the CFL, FFL and BL of individual cross-bed sets result in contrasts of primary porosity evolution and development of secondary porosity between the subfacies. A correlation exists between a decreasing ratio of carbonate to quartz and increasing permeability.
5. Outcrop probe permeameter studies show a range in permeabilities of 0·5–20 D. On average, contrasts in permeability between the subfacies are 2:1·25:1 (CFL:FFL:BL).
6. Probe permeability contrasts between CFL, FFL and BL depend on pore size and mineralogical composition contrasts between the subfacies.

ACKNOWLEDGMENTS

Thanks are due to Margarita Diaz Molina of the Universidad Complutense in Madrid for her valuable discussions in the field and for her constructive comments on the manuscript. Professor K. J. Weber is kindly thanked for his critical reading of the typescript and encouragement. The helpful comments of Thea van de Graaff-Trouwborst and Evert van de Graaff were much appreciated. *Sedimentology* reviewers Andrew Hurst and Steve Ehrenberg are thanked for critical comments on the typescript. Suggestions from an anonymous referee were also appreciated.

REFERENCES

ARRIBAS, J. & ARRIBAS, M.E. (1991) Petrographic evidence of different provenance in two alluvial fan systems (Paleogene of the Northern Tajo Basin, Spain). In: *Developments in Sedimentary Provenance Studies* (Ed. by A. C. Morton, S. P. Todd & P. D. W. Haughton), *Spec. Publ. geol. Soc.*, **57**, 263–271.

VAN BAAREN, J.P. (1979) Quick-look permeability estimates using sidewall samples and porosity logs. In: *Proc S.P.W.L.A. 6th European Logging Conference*, London, March, pp. 1–11.

BEARD, D.C. & WEYL, P.K. (1973) Influence of texture on porosity and permeability of unconsolidated sand. *Bull. Am. Ass. petrol. Geol.*, **57**, 349–369.

CARMAN, P.C. (1937) Fluid flow through granular beds. In: *Trans. Inst. Chem. Eng.*, **15**, 150–166.

CHANDLER, M.A., KOCUREK, G., GOGGIN, D.J. & LAKE, L.W. (1989) Effects of stratification heterogeneity on permeabiality in eolian sandstone sequence, Page Sandstone, Northern Arizona. *Bull. Am. Ass. petrol. Geol.*, **55**, 307–309.

DIAZ MOLINA, M., ARRIBAS MOCOROA, J. & BUSTILLO REVUELTA, A. (1989) The Tórtola and Villalba de la Sierra fluvial fans: Late Oligocene–Early Miocene, Loranca Basin, Central Spain. In: *Guidebook for Fieldtrip 7, 4th Int. Conf. on Fluvial Sedimentology, Barcelona-Sitges*, (Ed. by C. Puigdefabregas). Servei Geologicde Catalunya.

DIAZ MOLINA, M., CAPOTE, R. & LOPEZ MARTINEZ, N. (1985) Wet fluvial fans of the Loranca Basin (Central Spain), channel models and distal bioturbated gypsum and chert. In: *Fieldtrip Guidebook, 6th Int. Ass. Sediment., Eur. Reg. Meeting, Lerida, Spain* (Ed. by M. D. Mila & J. Rossell), pp. 149–185. Institut d'estudis Illerdencs.

DREYER, T., SCHREIE, Å & Walderhaug, O. (1990) Minipermeameter-based study of permeability trends in channel sand bodies. *Bull. Am. Ass. petrol. Geol.*, **74**, 359–374.

EHRENBERG, S.N. (1990) Relationship between diagenesis and Reservoir Quality in sandstones of the Garn Formation, Halterbanken, mid-norwegian continental shelf. *Bull. Am. Ass. petrol. Geol.*, **74**, 1538–1558.

EIJPE, R. & WEBER, K.J. (1971) Minipermeameters for consolidated rock and unconsolidated sand. *Bull. Am. Ass. petrol. Geol.*, **55**, 307–309.

FOLK, R.L. (1980) *Petrology of Sedimentary Rocks.* Hemphill Publishing Company, Austin, TX.

GIBBONS, K., HALVORSEN, C. & SIRING, E. (1991) Vertical and horizontal permeability variation within a sandstone reservoir based on minipermeameter data. In: *Proc. 1st Minipermeatry in Reserv. Studies Conference*, Edinburgh, 27–28 June, pp. 1–9.

GOGGIN, D.J., THRASHER, R.L. & LAKE, L.W. (1988) A theoretical and experimental analysis of minipermeameter response including gas slippage and high velocity flow effects. *In Situ*, **12**, 79–116.

GRINDHEIM, A.O. & AASEN, J.O. (1991) *An Evaluation of Homogenization Techniques for Absolute Permeability.* Lerkendal Petroleum Engineering Workshop, Trondheim.

HALVORSEN, C. & HURST, A. (1990) Principles, practice and application of laboratory minipermeametry. In: *Advances in Core Evaluation, Accuracy and Precision in Reserves Estimation* (Ed. by P. F. Worthington, pp. 521–549. Gordon & Breach.

HARTKAMP, C.A. (1993) *Permeability heterogeneity in cross-bedded sandstones. Impact on water/oil displacement in fluvial reservoirs.* PhD thesis, Krips-Repro, Meppel (in press).

HARTKAMP, C.A. & DONSELAAR, M.E. (1993) Permeability patterns in point-bar deposits: Tertiary Loranca Basin, Central Spain. In: *The Geological Modelling of Hydrocarbon Reservoirs* (Ed. by S. Flint & I. Bryant), *Spec. Publs Int. Ass. Sediment.*, **15**, 157–168.

HOPKINS, J.C., WOOD, J.M. & KRAUSE, F.F. (1991) Waterflood response of reservoirs in an estuarine valley fill: Upper Manville, G, U and W Pools, Little Bow Field, Alberta, Canada. *Bull. Am. Ass. petrol. Geol.*, **75**, 1064–1088.

HURST, A. & ROSVOLL, K. (1991) Permeability variations in sandstones and their relationship to sedimentary structures. In: *Reservoir Characterisation II* (Ed. L. W. Lake, H. B. Carroll, Jr & T. C. Wesson), pp. 116–196. Academic Press, San Diego, CA.

INGERSOLL, R.V. (1983) Petrofacies and provenance of a late Mesozoic forearc basin, northern and central California. *Bull. Am. Ass. petrol. Geol.*, **67**, 1125–1142.

JENSEN, J.L. (1990) A model for small-scale permeability measurement with applications to reservoir characterization. In: *Proc. Soc. Petrol. Engineers Symposium on Enhanced Oil Recovery*, Tulsa, OK, **SPE 20265**, 891–900.

JENSEN, L.J., HINKLEY, D.V. & LAKE, L.W. (1987) A statistical study of reservoir permeability: Distributions, correlations and averages. *Soc. Petrol. Eng. Form. Eval.*, December, 461–468.

JOPLIN, A.V. (1965) Laboratory study of the distribution of grain sizes in cross-bedded deposits. In: *Primary Sedimentary Structures and Their Hydrodynamic Interpretation* (Ed. by G. V. Middleton), *Spec. Publ. Soc. Econ. paleont. Miner.*, **12**, 53–65.

KOZENY, J. (1927) Uber kapillare leitung des wassers in boden. *Sitzber Akad. Wiss. Wien, Math. Naturw. Klasse, Abt. IIA*, **136**, 271–306.

MITRA, S. & BEARD, W.E. (1980) Theoretical models of porosity reduction by pressure solution for well-sorted sandstones. *J. sedim. Petrol.*, **50**, 1347–1360.

PETTIJOHN, F.J., POTTER, P.E. & SIEVER, R. (1973) *Sand and Sandstone*. Springer-Verlag, New York.

PITTMAN, E.D. (1979) Porosity, diagenesis and productive capability of sandstone reservoirs. In: *Aspects of Diagenesis* (Ed. by P. A. Scholle & P. R Schluger. *Spec. Publ. Soc. Econ. paleont. Miner.*, **26**, 159–173.

RITTENHOUSE, G. (1971) Mechancial compaction of sands containing different percentages of ductile grains: a theoretical approach. *Bull. Am. Ass. petrol. Geol.*, **55**, 92–96.

SCHMIDT, V. & MCDONALD, D.A. (1979) The role of secondary porosity in the course of sandstone diagenesis. In: *Aspects of Diagenesis* (Ed. by P. A. Scholle & P. R. Schluger), *Spec. Publ. Soc. Econ. paleont. Miner.*, **26**, 175–207.

SUTHERLAND, W.J., HALVORSEN, C., HURST, A., MCPHEE, C.A., ROBERTSON, G., WHATTLER, P.R. & WORTHINGTON, P.F. (1991) Recommended practice for probe permeametry. In: *Proc. Minipermeatry in Reserv. Studies Conference*, Edinburgh, 27–28 June, pp. 1–26.

TYLER, N., BARTON, M.D. & FINLEY, R.J. (1991) Outcrop characterization of flow unit and seal properties and geometries, Ferron Sandstone, Utah. In: *Proc. 66th Soc. Petrol. Engineers Annual Technical Conference and Exhibitions*, Dallas, 6–9 October, **SPE 22670**, 127–134.

ZUFFA, G.G. (1980) Hydrid arenites: their composition and classification. *J. sedim. Petrol.*, **50**, 21–29.